

Data-driven modeling of a four-dimensional stochastic projectile system

Yong Huang(黄勇) and Yang Li(李扬)

Citation: Chin. Phys. B, 2022, 31 (**7**): 070501. DOI: 10.1088/1674-1056/ac4e0d
Journal homepage: http://cpb.iphy.ac.cn; http://iopscience.iop.org/cpb

What follows is a list of articles you may be interested in

Multifractal analysis of the software evolution in software networks

Meili Liu(刘美丽), Xiaogang Qi(齐小刚), and Hao Pan(潘浩)
Chin. Phys. B, 2022, 31 (**3**): 030501. DOI: 10.1088/1674-1056/ac1b8a

Stability analysis of hydro-turbine governing system based on machine learning

Yuansheng Chen(陈元盛) and Fei Tong(仝飞)
Chin. Phys. B, 2021, 30 (**12**): 120509. DOI: 10.1088/1674-1056/ac04a9

Complex network perspective on modelling chaotic systems via machine learning

Tong-Feng Weng(翁同峰), Xin-Xin Cao(曹欣欣), and Hui-Jie Yang(杨会杰)
Chin. Phys. B, 2021, 30 (**6**): 060506. DOI: 10.1088/1674-1056/abd9b3

Nonlinear dynamics of a classical rotating pendulum system with multiple excitations

Ning Han(韩宁) and Pei-Pei Lu(鲁佩佩)
Chin. Phys. B, 2020, 29 (**11**): 110502. DOI: 10.1088/1674-1056/ab9df2

Exploring the relationship between fractal features and bacterial essential genes

Yong-Ming Yu(余永明), Li-Cai Yang(杨立才), Qian Zhou(周茜), Lu-Lu Zhao(赵璐璐), Zhi-Ping Liu(刘治平)
Chin. Phys. B, 2016, 25 (**6**): 060503. DOI: 10.1088/1674-1056/25/6/060503

Data-driven modeling of a four-dimensional stochastic projectile system

Yong Huang(黄勇)[1] and Yang Li(李扬)[2,†]

[1] *School of Energy and Power Engineering, Nanjing University of Science and Technology, Nanjing* 210094, *China*
[2] *School of Automation, Nanjing University of Science and Technology, Nanjing* 210094, *China*

(Received 28 November 2021; revised manuscript received 16 January 2022; accepted manuscript online 24 January 2022)

The dynamical modeling of projectile systems with sufficient accuracy is of great difficulty due to high-dimensional space and various perturbations. With the rapid development of data science and scientific tools of measurement recently, there are numerous data-driven methods devoted to discovering governing laws from data. In this work, a data-driven method is employed to perform the modeling of the projectile based on the Kramers–Moyal formulas. More specifically, the four-dimensional projectile system is assumed as an Itô stochastic differential equation. Then the least square method and sparse learning are applied to identify the drift coefficient and diffusion matrix from sample path data, which agree well with the real system. The effectiveness of the data-driven method demonstrates that it will become a powerful tool in extracting governing equations and predicting complex dynamical behaviors of the projectile.

Keywords: data-driven modeling, machine learning, projectile systems, Kramers–Moyal formulas

PACS: 05.10.–a, 05.10.Gg, 05.40.–a, 02.30.Zz **DOI:** 10.1088/1674-1056/ac4e0d

1. Introduction

Motion of a projectile is generally influenced by all sorts of forces and fluctuations in practical case. Its dynamical modeling based on classical mechanics is therefore not always accurate enough, and the analysis of its dynamical behaviors is not very reliable consequently. Fortunately, there are more and more available observable, experimental or simulated data in the projectile system with the development of the scientific tools and simulation capabilities. Thus, how to discover the governing laws of the projectile from data is of much importance in engineering fields.

Recently, many researchers have proposed various data-driven methods to extract the governing equations of complex nonlinear phenomena. For instance, the sparse identification of nonlinear dynamics method was devised to learn the deterministic ordinary[1,2] or partial[3–5] differential equations from time series data. Then, Boninsegna *et al.*[6] extended this approach to extract stochastic dynamical systems with Gaussian noise via Kramers–Moyal formulas. Li and Duan[7,8] made further efforts to propose the non-local Kramers–Moyal formulas and developed a data-driven approach to find the stochastic differential equations with both (Gaussian) Brownian motion and (non-Gaussian) Lévy motion from sample path data. The theory of Koopman operator can also be used to discover the deterministic and stochastic differential equations from data.[9–11] There are also some data-driven methods based on neural networks to learn dynamical systems from sample paths.[12–15] Additionally, some researchers are devoted to developing techniques to extract the dynamical behaviors such as mean exit time[16,17] and most probable path.[18,19]

Compared with the Koopman operator method, the neural network method and many other methods for system identification, the sparse learning based on the Kramers–Moyal formulas used in this study has the advantages that its computation speed is very fast and it is easy to program. Thus, in this paper we aim to apply the data-driven method based on the Kramers–Moyal formulas to the projectile systems. The article is arranged as follows. In Section 2, we describe the projectile systems and present its Itô stochastic differential equation. In Section 3, we introduce the Kramers–Moyal formulas and show the numerical method to learn the drift and diffusion terms for this system from simulated sample path data. Section 4 exhibits the comparison of the identification results and the real system. Finally, the conclusions are presented in Section 5.

2. Projectile systems

In order to generalize the data-driven method to the projectile systems, we simulate some sample path data based on the known model and identify the stochastic dynamical system from the data in this work. Formally, the angle motion equation of the projectile has the following form:[20]

$$\begin{aligned}
\dot{\delta}_1 &= \omega_\zeta \cos\delta_2 + \omega_\zeta \sin\delta_2 \tan\delta_2 \\
&\quad - \frac{1}{2mv}\rho v^2 S c_y' \cdot \sin\delta_1 \cos\delta_2, \\
\dot{\delta}_2 &= -\omega_\eta - \frac{1}{2mv\cos\delta_1}\rho v^2 S c_y' \sin\delta_2, \\
\dot{\omega}_\eta &= -\frac{C}{A}\omega_\xi \omega_\zeta + \omega^2 \zeta \tan\delta_2
\end{aligned}$$

†Corresponding author. E-mail: liyangbx5433@163.com

© 2022 Chinese Physical Society and IOP Publishing Ltd

$$
\begin{aligned}
&+\frac{1}{2A}\rho v^2 Sl\left(-m'_z\sin\delta_2\cos\delta_1-\left(\frac{l}{v}\right)m'_{zz}\omega_\eta\right.\\
&\left.+\left(\frac{\omega_\xi d}{v}\right)m''_y\sin\delta_1\right),\\
\dot{\omega}_\zeta &= \frac{C}{A}\omega_\xi\omega_\eta-\omega_\eta\omega_\zeta\tan\delta_2\\
&+\frac{1}{2A}\rho v^2 Sl\left(m'_z\sin\delta_1-\left(\frac{l}{v}\right)m'_{zz}\omega_\zeta\right.\\
&\left.+\left(\frac{\omega_\xi d}{v}\right)m''_y\sin\delta_2\cos\delta_1\right),
\end{aligned}
\tag{1}
$$

where $m''_y = m_{y0}+m_{y2}\left((\sin\delta_1)^2(\cos\delta_2)^2+(\sin\delta_2)^2\right)$.

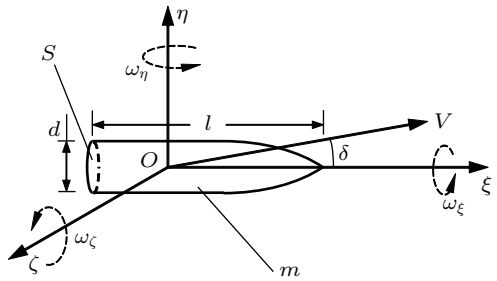


Fig. 1. The model of the projectile system.

Here, ξ, η and ζ denote the three axes of the projectile coordinate system, $O\xi$ indicates the direction of the projectile axis, $O\eta$ points upwards and is perpendicular to $O\xi$, and $O\zeta$ is perpendicular to the plane $O\xi\eta$ pointing right. The state variables ω_η and ω_ζ represent rotational angular velocity corresponding to η and ζ axes, respectively. The other two variables δ_1 and δ_2 indicate the vertical and horizontal components of the attack angle δ, which is the angle between the projectile axis and its velocity. The model of the projectile system with the axes and parameters is visualized in Fig. 1. The structure and aerodynamic parameters in the equation are listed in Tables 1 and 2, respectively.

Table 1. Structure parameters.

m (kg)	C (kg·m^2)	A (kg·m^2)	S (m^2)	l (m)	d (m)
44.2	0.12466	30.627	0.01269	2.7	0.122

Table 2. Aerodynamic parameters.

ω_ξ (rad/s)	c'_y	m'_z	m'_{zz}	m_{y0}	m_{y2}	ρ (kg/m^3)
79.0064	6.5	–1.3546	0.46	–5.8	30	0.68

The variable v denotes the velocity of the projectile during its flight in air, which can be easily influenced in general. In consideration of the random disturbances of air, the speed is assumed as $v=\bar{v}+\xi_t$, where $\bar{v}=1012.3$ m/s and the scalar stochastic process ξ_t is a white Gaussian noise satisfying $\mathbb{E}[\xi_t]=0$ and $\mathbb{E}[\xi_t\xi_s]=2\kappa\delta(t-s)$. The noise intensity is chosen as $\kappa=50$ in the following computation.

Note that there exist some nonlinear terms about noise in Eq. (1). After the expansion of these nonlinear terms and neglecting of the higher order terms, we reduce it as the following standard Itô stochastic differential equation:

$$
\dot{X}_t = b(X_t)+\sigma(X_t)\xi_t, \tag{2}
$$

where the random vector $X_t=[\delta_1,\delta_2,\omega_\eta,\omega_\zeta]^{\mathrm{T}}$, the drift coefficient

$$
b(X_t)=\begin{bmatrix}
\omega_\zeta\cos\delta_2+\omega_\zeta\sin\delta_2\tan\delta_2-\frac{1}{2m\bar{v}}\rho\bar{v}^2Sc'_y\cdot\sin\delta_1\cos\delta_2\\
-\omega_\eta-\frac{1}{2m\bar{v}\cos\delta_1}\rho\bar{v}^2Sc'_y\sin\delta_2\\
-\frac{C}{A}\omega_\xi\omega_\zeta+\omega^2{}_\zeta\tan\delta_2+\frac{1}{2A}\rho\bar{v}^2Sl\left(-m'_z\sin\delta_2\cos\delta_1-\left(\frac{l}{\bar{v}}\right)m'_{zz}\omega_\eta+\left(\frac{\omega_\xi d}{\bar{v}}\right)m''_y\sin\delta_1\right)\\
\frac{C}{A}\omega_\xi\omega_\eta-\omega_\eta\omega_\zeta\tan\delta_2+\frac{1}{2A}\rho\bar{v}^2Sl\left(m'_z\sin\delta_1-\left(\frac{l}{\bar{v}}\right)m'_{zz}\omega_\zeta+\left(\frac{\omega_\xi d}{\bar{v}}\right)m''_y\sin\delta_2\cos\delta_1\right)
\end{bmatrix}, \tag{3}
$$

and the diffusion coefficient $a=\sigma\sigma^{\mathrm{T}}$ with the function σ,

$$
\sigma(X_t)=\begin{bmatrix}
-\frac{1}{2m}\rho Sc'_y\cdot\sin\delta_1\cos\delta_2\\
-\frac{1}{2m\cos\delta_1}\rho Sc'_y\sin\delta_2\\
\frac{1}{2A}\rho Sl\left(-2\bar{v}m'_z\sin\delta_2\cos\delta_1-lm'_{zz}\omega_\eta+\omega_\xi dm''_y\sin\delta_1\right)\\
\frac{1}{2A}\rho Sl\left(2\bar{v}m'_z\sin\delta_1-lm'_{zz}\omega_\zeta+\omega_\xi dm''_y\sin\delta_2\cos\delta_1\right)
\end{bmatrix}. \tag{4}
$$

3. Theory and method

According to the Fokker–Planck equation corresponding to stochastic differential equation (2), the drift and diffusion coefficients dominate the probabilistic structure of the solution process X_t.[21] Therefore, the discovery of the stochastic governing laws from sample path data completely depends on the identification of the drift and diffusion terms.

The Kramers–Moyal formulas can be used to extract the underlying stochastic dynamical systems from data, which express the drift and diffusion coefficients in terms of the sample paths of the solution process.[6,22] For our systems, these equa-

tions can be formulated as

$$\begin{aligned} b^i(x) &= \lim_{t\to 0}\mathbb{E}\left[t^{-1}\left(X_t^i - x^i\right)|X_0 = x\right], \\ & \quad i = 1,2,3,4, \\ a^{ij}(x) &= \lim_{t\to 0}(2\kappa)^{-1}\mathbb{E}\left[t^{-1}\left(X_t^i - x^i\right)\left(X_t^j - x^j\right)|X_0 = x\right], \\ & \quad i,j = 1,2,3,4, \end{aligned} \tag{5}$$

where $b^i(x)$ denotes i-th component of the drift vector $b(x)$ in Eq. (3), and $a^{ij}(x)$ indicates ij-th component of the diffusion matrix $a(x)$. Then the drift $b(x)$ and diffusion $a(x)$ can be estimated by approximately computing the limit expressions on the right-hand side in terms of sample path data of X_t.

Assume that there exists a pair of data sets for the stochastic process X_t containing M elements, respectively,

$$\begin{aligned} X &= [x_1, x_2, \ldots, x_M], \\ Y &= [y_1, y_2, \ldots, y_M], \end{aligned} \tag{6}$$

where every y_i is the image point of x_i after a small evolution time h for $i = 1,2,\ldots,M$. In other words, Eq. (2) is integrated by numerical integral methods such as the Runge–Kutta method from initial point x_i to get y_i in time h. Note that the superscript in Eq. (5) denotes different component of vector or matrix and the subscript in Eq. (6) indicates different data. It is also necessary to choose a dictionary of basis functions $\Psi(x) = [\psi_1(x), \psi_2(x), \ldots, \psi_K(x)]$ to approximate the drift and diffusion terms. The results will be better if we seek as rich type of the basis functions as possible, while the amount of work is immense and polynomial basis functions are sufficiently accurate for most cases. Thus we select polynomial functions as the dictionary in this research.

Assume that the system has ergodic property and every component of the drift coefficient is estimated as $b^i(x) = \sum_{k=1}^K c_k^i \psi_k(x)$, $i = 1,2,3,4$. Moreover, the limit expressions on the left-hand side of Kramers–Moyal formulas can be approximated by finite differences. Above all, we can derive the following group of linear equations via Eqs. (5) and (6):

$$\begin{aligned} & Ac^i = B^i, \\ & A = \begin{bmatrix} \psi_1(x_1) & \cdots & \psi_K(x_1) \\ \vdots & \ddots & \vdots \\ \psi_1(x_M) & \cdots & \psi_K(x_M) \end{bmatrix}, \\ & B^i = h^{-1}\left[y_1^i - x_1^i, \ \ldots, \ y_M^i - x_M^i\right]^{\mathrm{T}}, \\ & c^i = \left[c_1^i, \ \ldots, \ c_K^i\right]^{\mathrm{T}}. \end{aligned} \tag{7}$$

This group of equations has no solution in general since the number of equations is usually far more than the number of variables due to enormous amounts of data. Then a least square method can be applied to deal with the minimization problem $\min_{c^i} \|Ac^i - B^i\|_2^2$, which yields the optimal solution

$$\widetilde{c}^i = (A^{\mathrm{T}}A)^{-1}(A^{\mathrm{T}}B^i). \tag{8}$$

The solution to Eq. (8) is generally very dense, which contains many non-dominant terms close to zero. For the sake of seeking the least coefficients without loss of reliability and avoiding overfitting, the sparse solution should be enforced by minimizing

$$\min_{c^i}\left(\|Ac^i - B^i\|_2^2 + \rho\|c^i\|_1\right), \tag{9}$$

where ρ indicates a positive Lagrange multiplier to control the degree of sparsity.

We can use the iterating thresholding algorithm to realize the sparse learning method (9).[1,6,7] First, we can choose an appropriate pre-defined threshold parameter λ as a sparsification knob. The magnitude of λ is usually chosen as about 0.1%–10% of the largest coefficient of c^i. After Eq. (8) being performed to obtain a non-sparse solution, we set the coefficients smaller than λ as zero and delete the corresponding basis functions. Then the regression problem is carried out on the remaining coefficients. The procedure is iterated until no coefficients are found smaller than λ.

Similarly, assume that every component of diffusion term is expressed as $a^{ij}(x) = \sum_{k=1}^K d_k^{ij}\psi_k(x)$, $i,j = 1,2,3,4$. Via the second equation of Kramers–Moyal formulas (5), we can derive the following group of equations:

$$\begin{aligned} & Ad^{ij} = B^{ij}, \\ & A = \begin{bmatrix} \psi_1(x_1) & \cdots & \psi_K(x_1) \\ \vdots & \ddots & \vdots \\ \psi_1(x_M) & \cdots & \psi_K(x_M) \end{bmatrix}, \\ & B^{ij} = h^{-1}\left[(y_1^i - x_1^i)(y_1^j - x_1^j), \ \ldots, \ (y_M^i - x_M^i)(y_M^j - x_M^j)\right]^{\mathrm{T}}, \\ & d^{ij} = \left[d_1^{ij}, \ \ldots, \ d_K^{ij}\right]^{\mathrm{T}}. \end{aligned} \tag{10}$$

The optimal solution of the least square problem $\min_{d^{ij}} \|Ad^{ij} - B^{ij}\|_2^2$ is obtained as

$$\widetilde{d}^{ij} = (A^{\mathrm{T}}A)^{-1}(A^{\mathrm{T}}B^{ij}). \tag{11}$$

The sparse learning method can also be applied in the estimation of the diffusion. Remark that we just need to compute 10 components for $i = 1,2,3,4$, $j = i,\ldots,4$ due to the symmetry of the diffusion matrix. The algorithm for identifying the drift coefficient and diffusion matrix is concluded in Table 3.

Remark that it is not unique to infer the coefficient $\sigma(x)$ in terms of the diffusion matrix $a(x)$. Via the symmetry of $a(x)$, the orthogonal matrix Q that is composed of the eigenvectors of $a(x)$ can diagonalize the diffusion matrix, i.e., $J = Q^{\mathrm{T}}aQ$ with the component in the diagonal $J_{ii} \geq 0$. Then $J = \left(Q^{\mathrm{T}}\sigma\right)\cdot\left(Q^{\mathrm{T}}\sigma\right)^{\mathrm{T}}$. Denoting $\sqrt{J}$ as the diagonal matrix with the diagonal component $\sqrt{J_{ii}}$, the matrix $Q\sqrt{J}$ is a solution to this equation. Note that for arbitrary orthogonal matrix T, the matrix $Q\sqrt{J}T$ is also a solution. Even so, they are statistically equivalent as they have the same Fokker–Planck equation for a given diffusion matrix.

Table 3. The algorithm for identifying the drift and diffusion terms from sample path data.

Algorithm: Identifying drift coefficient $b(x)$ and diffusion matrix $a(x)$ from sample path data
Input: Dictionary $\Psi(x)$, data sets X and Y, threshold λ.
1. Compute the matrix A, every vector B^i in Eq. (7) and B^{ij} in Eq. (10).
2. Calculate $\widetilde{c}^i$ and $\widetilde{d}^{ij}$ via Eqs. (8) and (11).
3. Delete the coefficients smaller than λ and corresponding basis functions in the dictionary.
4. Iterate step 1–3 until no coeffcient is smaller than λ.
Output: The optimal sparsity solution $\widetilde{c}^i$ and $\widetilde{d}^{ij}$.

4. Results

In the above section, we described the data-driven method to extract the stochastic dynamical systems from sample path data based on the Kramers–Moyal formulas. We now show the effectiveness of this technique applied on the projectile system introduced in Section 2.

First, we choose $M = 10^4$ initial points to construct the data set X, which are uniformly and randomly distributed in the region $[-1,1]\times[-1,1]\times[-1,1]\times[-1,1]$. Given the time step $h = 0.0001$, the image data set Y is integrated via Euler scheme of the stochastic system (2). The dictionary Ψ of basis functions is selected as the polynomial functions up to order 3, which contains 35 terms since the system is four-dimensional. Based on these preliminaries, we can compute the matrix A and vectors B^i, B^{ij} in Eqs. (7) and (10).

Via the least square method and sparse learning, all the components of the drift and diffusion coefficients are evaluated as the linear combination of the polynomial basis functions. Since the system is four-dimensional, it is impossible to show these functions intuitively in the figures. Thus we portray them as two-dimensional surfaces by fixing two state variables.

The learned and true functions of four components of the drift coefficient are shown in Figs. 2–5, respectively. In every figure, the top panels denote the learned results and the bottom panels correspond to the true functions. The four columns of the figures indicate the cases with (i) $\omega_\eta = 0.5$, $\omega_\zeta = 0.5$; (ii) $\omega_\eta = -0.5$, $\omega_\zeta = -0.5$; (iii) $\delta_1 = 0.5$, $\delta_2 = 0.5$; (iv) $\delta_1 = -0.5$, $\delta_2 = -0.5$, respectively. It is seen that the estimation results agree well with the true functions of the drift terms. The third and fourth components have a small error but still within an acceptable range. This error stems from the fact that the magnitude of the two components is much larger than the first two. A coordinate transformation can lead to more accurate results.

As mentioned above, there are 10 elements of the diffusion matrix that need to be identified from data due to the symmetry. For the sake of simplification, we just present the diagonal elements a_{11}, a_{22}, a_{33} and a_{44} for the case of $\omega_\eta = 0.5$, $\omega_\zeta = -0.5$ in Fig. 6. The results show that the accuracy of the approximation of the diffusion term is not as good as the one for the drift coefficient, while it can still capture the dynamical structures. It seems that the errors for a_{11} and a_{22} are relatively larger. This is because the magnitude of them is too small to be sufficiently accurate. Above all, the identification of the stochastic dynamical system is consistent enough with the real model.

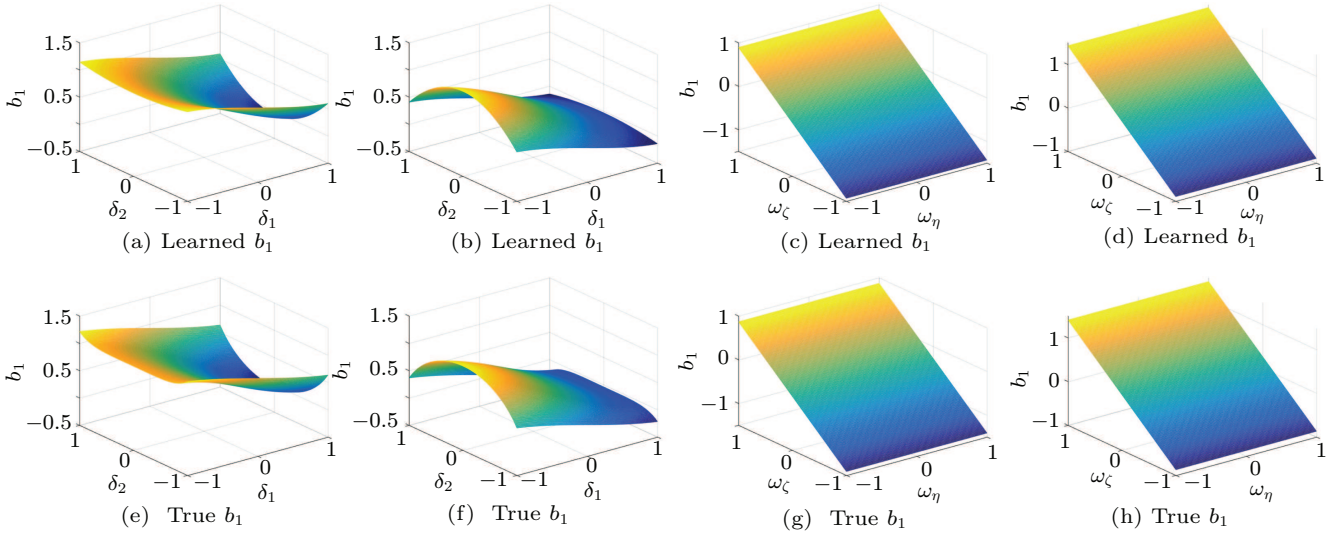


Fig. 2. Comparison between learned and true function of the first component of the drift coefficient: (a) and (e) $\omega_\eta = 0.5$, $\omega_\zeta = 0.5$; (b) and (f) $\omega_\eta = -0.5$, $\omega_\zeta = -0.5$; (c) and (g) $\delta_1 = 0.5$, $\delta_2 = 0.5$; (d) and (h) $\delta_1 = -0.5$, $\delta_2 = -0.5$.

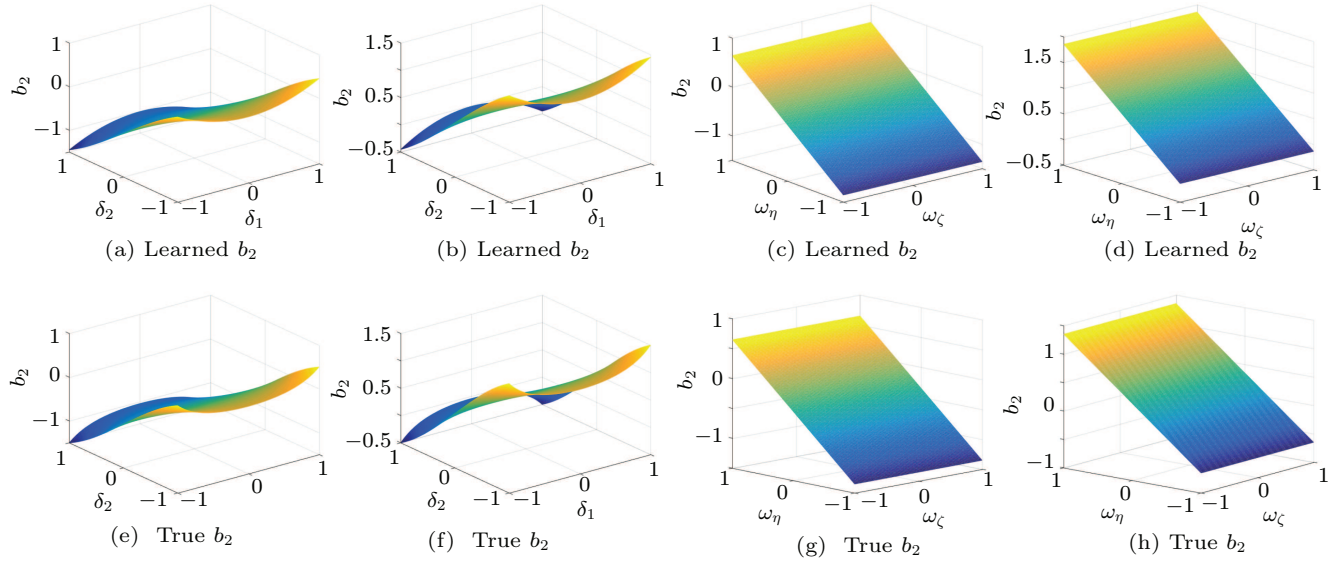


Fig. 3. Comparison between learned and true function of the second component of the drift coefficient: (a) and (e) $\omega_\eta = 0.5$, $\omega_\zeta = 0.5$; (b) and (f) $\omega_\eta = -0.5$, $\omega_\zeta = -0.5$; (c) and (g) $\delta_1 = 0.5$, $\delta_2 = 0.5$; (d) and (h) $\delta_1 = -0.5$, $\delta_2 = -0.5$.

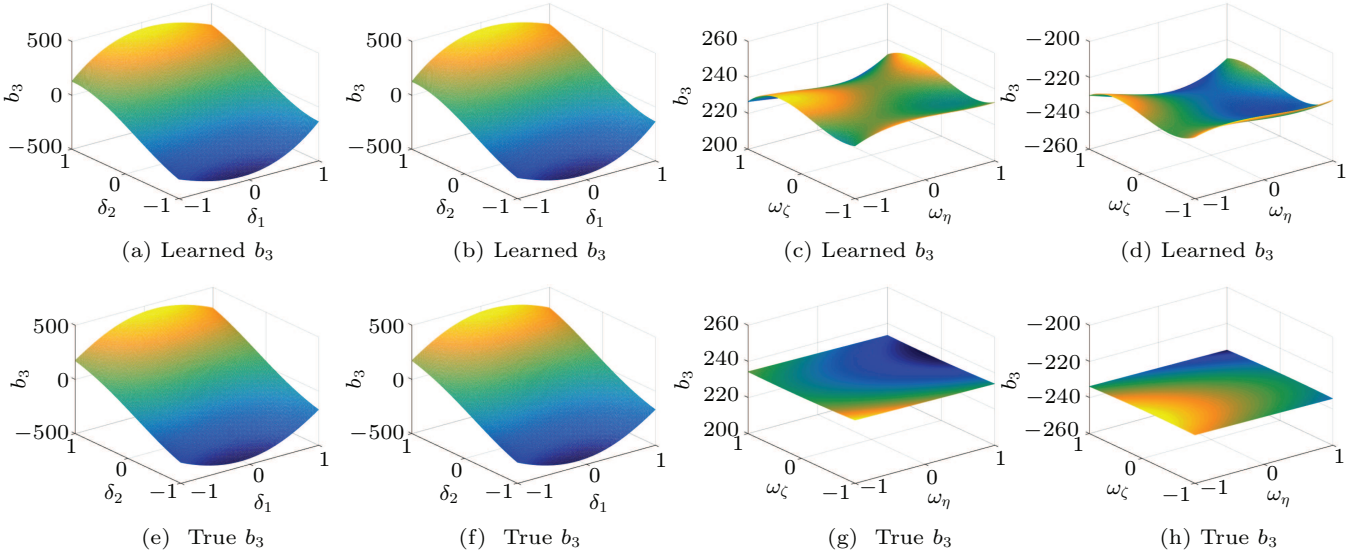


Fig. 4. Comparison between learned and true function of the third component of the drift coefficient: (a) and (e) $\omega_\eta = 0.5$, $\omega_\zeta = 0.5$; (b) and (f) $\omega_\eta = -0.5$, $\omega_\zeta = -0.5$; (c) and (g) $\delta_1 = 0.5$, $\delta_2 = 0.5$; (d) and (h) $\delta_1 = -0.5$, $\delta_2 = -0.5$.

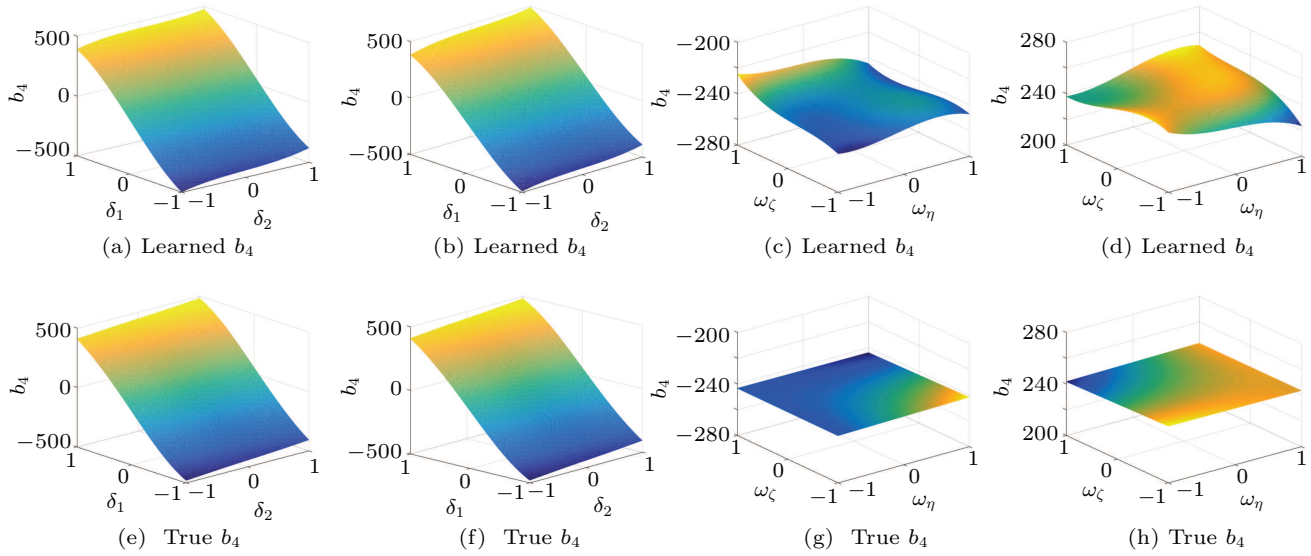


Fig. 5. Comparison between learned and true function of the fourth component of the drift coefficient: (a) and (e) $\omega_\eta = 0.5$, $\omega_\zeta = 0.5$; (b) and (f) $\omega_\eta = -0.5$, $\omega_\zeta = -0.5$; (c) and (g) $\delta_1 = 0.5$, $\delta_2 = 0.5$; (d) and (h) $\delta_1 = -0.5$, $\delta_2 = -0.5$.

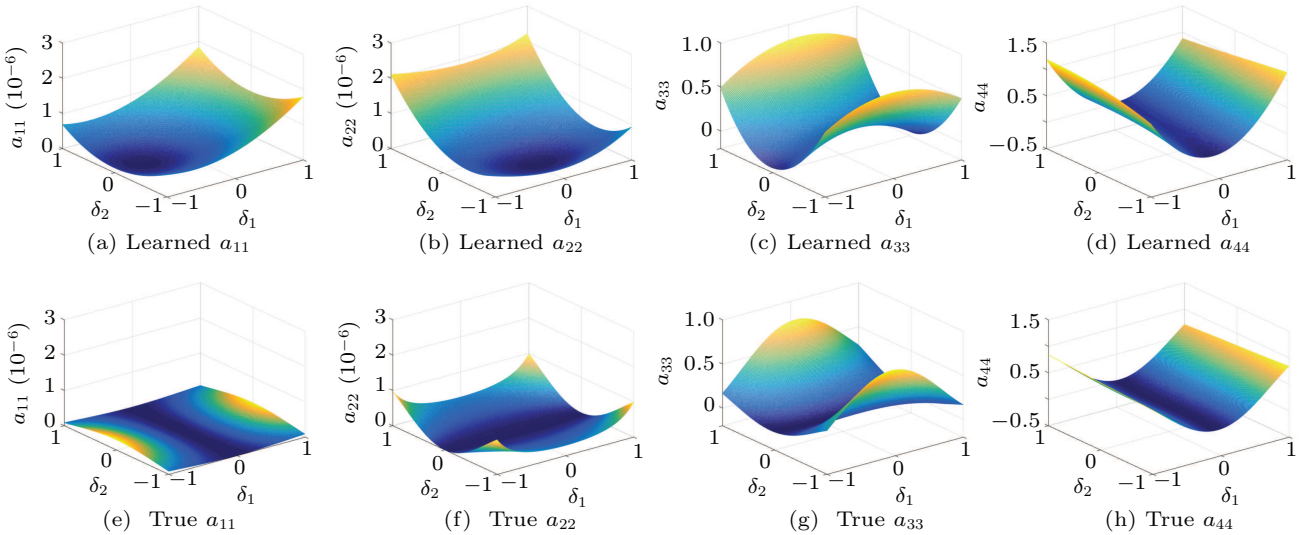


Fig. 6. Comparison between learned and true function of the diagonal elements a_{11}, a_{22}, a_{33} and a_{44} of the diffusion matrix for $\omega_\eta = 0.5$, $\omega_\zeta = -0.5$.

5. Conclusion

In summary, we have employed a data-driven method based on the Kramers–Moyal formulas to extract the stochastic model for the four-dimensional projectile systems from simulated sample path data. Specifically, the projectile system is assumed as an Itô stochastic differential equation. Then the least square method and sparse learning are applied to compute the drift coefficient and diffusion matrix, which are sufficiently accurate to the true functions. The effective approximation of the learned model to the real one implies that the data-driven method can be well applied to the projectile systems. Therefore, given the measurable time-series data, we can establish the governing equations for the projectile in the engineering field. This fact demonstrates that it has many applications in practical problems. For example, the learned model of the projectile can be used to analyze its dynamical responses so that we can improve the performances of the projectile by adjusting its shape and structure.

Acknowledgement

This research was supported by the Six Talent Peaks Project in Jiangsu Province, China (Grant No. JXQC-002).

Data availability statement

The data that support the findings of this study are openly available in GitHub.

References

[1] Brunton S L, Proctor J and Kutz J 2016 *Proc. Natl. Acad. Sci. USA* **113** 3932
[2] Champion K, Lusch B, Kutz J N and Brunton S L 2019 *Proc. Natl. Acad. Sci. USA* **116** 22445
[3] Schaeffer H, Caisch R, Hauck C D and Osher S 2013 *Proc. Natl. Acad. Sci. USA* **110** 6634
[4] Rudy S, Alla A, Brunton S L and Kutz J N 2019 *SIAM J. Appl. Dyn. Systems* **18** 643
[5] Lee S, Kooshkbaghi M, Spiliotis K, Siettos C I and Kevrekidis I G 2020 *Chaos* **30** 013141
[6] Boninsegna L, Nüske F and Clementi C 2018 *J. Chem. Phys.* **148** 241723
[7] Li Y and Duan J 2021 *Physica D* **417** 132830
[8] Li Y and Duan J 2022 *J. Stat. Phys.* **186** 30
[9] Williams M O, Kevrekidis I G and Rowley C 2015 *J. Nonlinear Sci.* **25** 1307
[10] Klus S, Nüske F, Peitz S, Niemann J H, Clementi C and Schütte C 2020 *Physica D* **406** 132416
[11] Lu Y and Duan J 2020 *Chaos* **30** 093110
[12] Raissi M, Perdikaris P and Karniadakis G 2019 *J. Comput. Phys.* **378** 686
[13] Chen X, Yang L, Duan J and Karniadakis G E 2021 *SIAM J. Sci. Comput.* **43** B811
[14] Lu Y, Li Y and Duan J 2021 arXiv:2108.12570 [math.DS]
[15] Chen R T Q, Rubanova Y, Bettencourt J and Duvenaud D 2018 *Advances in Neural Information Processing Systems* (Curran Associates, Inc.) Vol. 31
[16] Wu D, Fu M and Duan J 2019 *Chaos* **29** 093122
[17] Zhang Y, Duan J, Jin Y and Li Y 2020 *Chaos* **30** 113112
[18] Li Y, Duan J and Liu X 2021 *Phys. Rev. E* **103** 012124
[19] Dai M, Gao T, Lu Y, Zheng Y and Duan J 2020 *Chaos* **30** 113124
[20] Han Z P 2008 *Exterior Ballistics for projectiles* (Beijing: Beijing University of Technology Press) (in Chinese)
[21] Duan J 2015 *An Introduction to Stochastic Dynamics* (New York: Cambridge University Press)
[22] M Reza Rahimi Tabar 2019 *Analysis and Data-Based Reconstruction of Complex Nonlinear Dynamical Systems* (Springer) 11